Multistage Rotor-Stator Spinning Disc Reactor

Marco Meeuwse, John van der Schaaf and Jaap C. Schouten
Laboratory of Chemical Reactor Engineering, Dep. of Chemical Engineering and Chemistry, Eindhoven University of Technology, 5600 MB Eindhoven, The Netherlands

DOI 10.1002/aic.12586
Published online March 22, 2011 in Wiley Online Library (wileyonlinelibrary.com).

The scale up of a rotor-stator spinning disc reactor by stacking single stage rotor-stator units in series is demonstrated. The gas-liquid mass transfer per stage is equal to the mass transfer in a single stage spinning disc reactor. The pressure drop per stage increases with increasing rotational disc speed and liquid flow rate. The pressure drop is more than a factor 2 higher for gas-liquid flow than for liquid flow only, and is up to 0.64 bar at 459 rad s^{-1}. The high mass and heat transfer coefficients in the (multistage) rotor-stator spinning disc reactor make it especially suitable for reactions with dangerous reactants, highly exothermic reactions and reactions where selectivity issues can be solved by high mass transfer rates. Additionally, the multistage rotor-stator spinning disc reactor mimics plug flow behavior, which is beneficial for most processes. © 2011 American Institute of Chemical Engineers *AIChE J,* 58: 247–255, 2012
Keywords: spinning disc reactor, rotor-stator, mass transfer, multi-phase flow, reactor analysis

Introduction

The productivity of reactors for multiphase processes is often limited by the rate of the mass transfer steps, from the gas to the liquid and from the liquid to the solid (catalyst). A higher mass transfer rate can thus lead to a higher productivity, or to a smaller reactor with the same productivity. Additionally, the mass transfer rates can influence the selectivity of reactions.

The gas–liquid mass transfer coefficient ($k_{GL}a_{GL}$) is the product of the gas-liquid interfacial area (a_{GL}) and the gas-liquid mass transfer coefficient (k_{GL}). The former is commonly increased by increasing the surface area where liquid has to flow over, e.g., in a falling film reactor or in a (structured) packing, or by decreasing the gas bubble size, which is e.g., done by a stirrer. The gas-liquid mass transfer coefficient often depends on the energy dissipation rate and can thus be increased by increasing the flow rate, e.g., in a packed bed reactor, or by dissipating energy into the reactor directly, e.g., by using a stirrer.

Correspondence concerning this article should be addressed to J. C. Schouten at j.c.schouten@tue.nl.

The rotor-stator spinning disc reactor is a new type of multiphase reactor, which shows high mass transfer rates compared with conventional equipment[1–3] (Meeuwse et al., submitted). The rotor-stator spinning disc reactor consists of a rotating disc, enclosed in a cylindrical housing. The distance between the rotor and the reactor wall is small, commonly 1 mm. A high velocity gradient is present in the gap between the rotor and the stator, which acts as a shear force which breaks up gas bubbles, leading to a high gas-liquid interfacial area. The high energy input in the system, due to the rotation of the disc, leads to small turbulent eddies, with a high velocity, that increase the gas-liquid and liquid-solid mass transfer coefficients. Two different configurations of the rotor-stator spinning disc reactor have been investigated. In the first case, gas is injected through an orifice in the bottom stator, near the rim of the rotor; liquid is injected from the top of the reactor[1] (Meeuwse et al., submitted). In the second case, gas and liquid are fed together to the spinning disc reactor.[2]

Meeuwse et al.[1] describe the gas-liquid mass transfer in case of a single gas inlet in the bottom stator. The gas bubbles are sheared off at the gas inlet, due to the velocity gradient; the gas bubble size decreases with increasing rotational disc speed, leading to an increase in gas-liquid mass transfer.[1] The volumetric gas-liquid mass transfer coefficient

increases with increasing rotor radius, up to 2.5 m_L^3 m_R^{-3} s^{-1}, at a rotational disc speed of 209 rad s^{-1}, using a rotor with 0.135 m radius and 1 mm rotor-stator distance (Meeuwse et al., submitted). The energy dissipation rate, however, increases more than the mass transfer rate; scaling up by stacking multiple rotor-stator units in series is therefore, from energetic point of view, preferred over scaling up in rotor size. For scaling up by numbering up the reactor configuration with the gas inlet in the bottom stator, however, a complicated gas (re)distribution system may be needed.

In the other configuration used, gas and liquid are both fed to the top of the reactor,[2] as shown schematically in Figure 1. The gas-liquid dispersion which enters the reactor separates, on top of the rotor a liquid film will form, with the gas phase present between this liquid film and the top stator; this is called the film flow region. Small gas bubbles are sheared off near the rim of the rotor. The rest of the reactor, the dispersed flow region, is thus filled with small gas bubbles dispersed in the liquid. The volumetric mass transfer coefficient multiplied by the reactor volume ($k_{GL}a_{GL}V_R$) in this configuration is up to a factor 2 higher than in the case of the single gas inlet in the bottom stator. This is mainly because the whole reactor volume is used, contrary to the case with the gas inlet in the stator, where only the region between the rotor and the bottom stator contributes to the mass transfer. Near the center of the reactor the gas bubbles coalesce to larger bubbles, a gas-liquid dispersion leaves the reactor via the exit in the bottom. If the gas-liquid dispersion leaving the dispersed flow region is added to a next stage, it is therefore expected that the same flow regime, i.e., the film flow and the dispersed flow, is obtained. Scaling up this concept to a multistage spinning disc reactor is thus less complicated, since no gas redistribution system is needed.

The scale up of a reactor is an important step toward an industrial process. The reactor volume has to be increased, either to increase the residence in the reactor, or to increase the production capacity. In this study, the rotor-stator spinning disc reactor is scaled up by stacking multiple (up to 3) rotor-stator stages in series, where the rotors are mounted on a common axis. It is expected that the same flow behavior is obtained as in the single stage rotor-stator spinning disc reactor. A gas-liquid dispersion is fed to the reactor, which immediately separates in the film flow and the gas phase on top. At the exit of the reactor the gas bubbles coalesce to larger gas bubbles, and a similar gas-liquid dispersion is formed as which is fed. It is thus highly probable that the same behavior will be present when fed to the next stage. The strategy to scale up by using rotor-stator stages in series is, for most reactions, preferred above scaling up in rotor size, since the mass transfer per unit of energy dissipation is higher. Additionally, in a multiple rotor-stator spinning disc reactor the liquid and the gas will mimic plug behavior. If necessary, the stages in the multistage spinning disc reactor can operate under different reaction conditions, e.g., temperatures and catalysts, and it can thus be used for multi-step synthesis. This study shows that the scale up by stacking multiple rotor-stator stages in series is a viable method to increase the residence time and/or the production capacity in the rotor-stator spinning disc reactor.

This study describes the multistage rotor-stator spinning disc reactor, with 2 or 3 rotor-stator stages, where the gas and the liquid are fed together to the first stage. It is compared with the single stage unit, to investigate whether the same flow regime, with the film flow region and the dispersed flow region, is obtained. This is done by quantifying the mass transfer rate in the dispersed flow region and comparing this to a single stage unit. Additionally, the energy dissipation rate and the pressure drop of this multistage rotor-stator spinning disc reactor are described. The last section summarizes the main advantages and disadvantages of the multistage spinning disc reactor and compares it with reactors commonly used in industry and gives a few examples of potential applications.

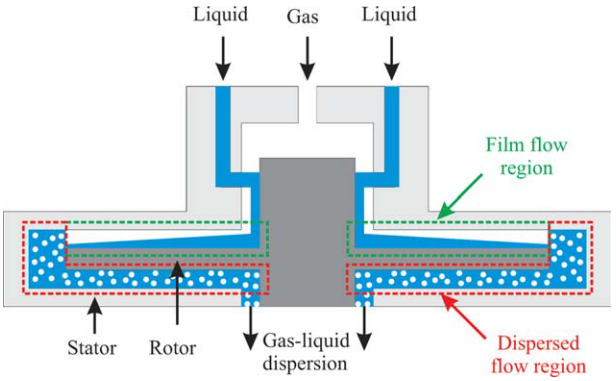

Figure 1. Schematic drawing of the concept of the rotor-stator spinning disc reactor with co-feeding of gas and liquid (not on scale).

Gas and liquid are added to the top of the reactor. The liquid flows as a thin film over the rotor; the gas phase is present above, this region is called the film flow region. Near the rim of the rotor, gas bubbles are sheared off. The region surrounding the rim of the rotor and the region between the rotor and the bottom stator, therefore has liquid as continuous phase, with small gas bubbles dispersed in it. This region is denoted as the dispersed flow region. A gas liquid dispersion leaves the reactor via the bottom outlet; it is expected that feeding this dispersion to the next stage will lead to the same flow behaviour. [Color figure can be viewed in the online issue, which is available at wiley onlinelibrary.com.]

Experimental

Experimental setup

Figure 2 shows a schematic representation of the multistage spinning disc reactor, which is made of stainless steel. It consists of an axis (radius 0.017 m) with 3 rotors attached to it, which has a maximum rotational disc speed of 470 rad s^{-1}. The radius of the rotors is 0.066 m, the inner reactor radius is 0.076 m, the radial distance between the rotor and the reactor wall is thus 0.01 m. The height of a stage is 8 mm, the thickness of the discs is 6 mm. The rotor-stator distance is thus 1 mm on both sides. The distance between the axis and the stator plates is 1 mm as well. The rotor size, the inner reactor radius, and the rotor-stator distance are the same as in the single stage rotor-stator spinning disc reactor.[1,2] Gas is injected at the top of the reactor, into a gas chamber. The liquid is injected by four channels (only two of them are shown in the drawing) onto the axis. The outlet of the reactor is on the bottom.

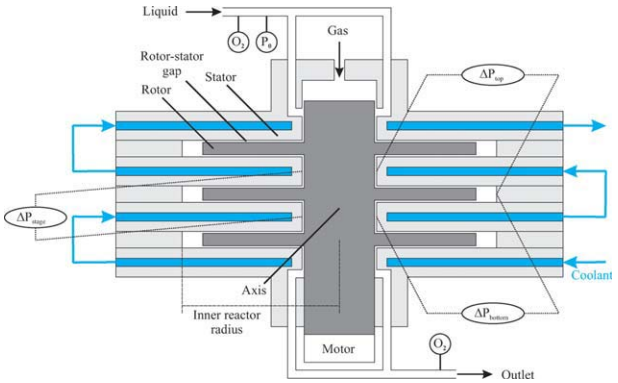

Figure 2. Schematic drawing of the 3-stage multistage spinning disc reactor.

The rotors are attached to an axis which has a maximum rotational speed of 470 rad s^{-1}. The radius of the rotors is 0.066 m and the inner reactor radius is 0.076 m. The axial rotor-stator distance is 1 mm. Gas and liquid are added to the reactor from the top, the gas-liquid dispersion leaves the reactor via the bottom. Cooling liquid (water in this study) flows through the hollow stators, countercurrently with the process fluids. The pressure differences as denoted in the drawing are measured using pressure sensors connected to the outer rim of the reactor. [Color figure can be viewed in the online issue, which is available at wileyonlinelibrary.com.]

The motor which drives the axis uses up to 2.5 kW of energy, of which most will be converted into heat. To keep the reactor temperature approximately constant, the heat has to be removed from the reactor: cooling liquid (tap water) continuously flows through the hollow stators. The stators contain redistribution walls on the inside, to increase the liquid velocity, and thus the heat transfer coefficient, on the coolant side. The stator walls are 5 mm thick. The coolant is fed to the bottom stator, at the outlet it is fed to the next stator. The coolant thus flows countercurrently with the process fluids.

The motor used to rotate the rotor is a SEW Eurodrive CFM71M. The torque is proportional to the current applied to the motor, which is measured. The torque with the motor running idle, i.e., without rotors, is subtracted from the total torque. The energy dissipation rate per unit volume of reactor follows from the torque:

$$E_d = \frac{\tau\omega}{V_R} \tag{1}$$

The gas-liquid mass transfer rates in this study are measured by the desorption of oxygen from water. The gas (nitrogen) and liquid (water) flow rates are controlled by a Bronkhorst gas mass flow controller and a Coriflow, respectively. The oxygen concentration at the inlet liquid and at the outlet is measured with Ocean Optics FOXY-R fiber optic sensors and an Avantes spectrometer. The oxygen sensors are calibrated as a function of temperature, which is measured simultaneously and ranges from 15 to 30°C. The gauge pressure (relative to atmospheric conditions) is measured in the inlet tube of the liquid, as well as at the rim of reactor Stage 2. Additionally, the pressure difference between the rim of Stage 1 and the rim of Stage 3 is measured. The differential pressures as indicated in Figure 2 are calculated from these pressures:

$$\Delta P_{stage} = \frac{P_0}{3} = \frac{P_1 - P_3}{2} \tag{2}$$

$$\Delta P_{top} = P_2 - 2\Delta P_{stage} \tag{3}$$

$$\Delta P_{bottom} = \Delta P_{top} + \Delta P_{stage} \tag{4}$$

A liquid flow rate of $2.7 \cdot 10^{-5}$ m^3 s^{-1} is fed to the reactor from a 2 dm^3 stirred vessel. The vessel is aerated to increase the oxygen concentration. The outlet liquid is recycled to the vessel. The cooling liquid is tap water of approximately 15°C. Nitrogen is used as the gas phase in the reactor, the flow rate is varied up to $3 \cdot 10^{-5}$ m^3 s^{-1} at normal flow conditions.

Gas-liquid mass transfer

Meeuwse et al.[2] described the gas-liquid mass transfer in a single stage spinning disc reactor, where gas and liquid are fed together to the bottom of the reactor. A liquid film is present on top of the rotor, the gas phase fills the rest of the region, see Figure 1. The liquid film is in plug flow behavior, the gas phase is assumed to be ideally mixed, since a recirculation of the gas is induced by the radial and tangential velocity of the liquid. A Sherwood correlation for the gas-liquid mass transfer coefficient on a spinning disc with a liquid film present is used for the calculation of the gas-liquid mass transfer coefficient in the film flow region[2,4,5]:

$$\overline{Sh} = 10.8 \cdot 10^{-4}\, Re^{0.94} C_w^{0.24} Sc^{\frac{1}{2}} \tag{5}$$

The gas-liquid interfacial area is the top area of the rotor divided by the volume of the film flow region:

$$a_{GL} = \frac{A_{top}}{V_F} = \frac{\pi R_D^2}{h\pi R_D^2} = \frac{1}{h} = 1 \cdot 10^3 m_i^2 m_R^{-3} \tag{6}$$

Small gas bubbles are sheared off from the gas phase in the film flow region, at the rim of the rotor. The region surrounding the rim of the rotor and the region between the rotor and the bottom stator is thus filled with gas bubbles dispersed in liquid, as shown schematically in Figure 1. The gas bubbles in the dispersed flow region flow radially inwards, due to the centrifugal force. No coalescence of gas bubbles is observed, and most of the gas bubbles have approximately the same residence time; the gas phase is thus assumed to be in plug flow. A recirculation of the liquid is induced by the rotation of the rotor,[2,6,7] the liquid phase in the dispersed flow region is therefore assumed to be ideally mixed.

A representation of the reactor model used for the combination of the film flow region and the dispersed flow region is shown in Figure 3, where the number of stages, N, is one. The oxygen concentrations are measured at the inlet and the outlet. The $k_{GL}a_{GL}$ in the film flow region is calculated from Eq. 5, the rest of the mass transfer thus occurs in the dispersed flow region. In this way the value of the volumetric gas-liquid mass transfer coefficient, $k_{GL}a_{GL}$, is obtained.

The same flow behavior is expected in the multistage spinning disc reactor ($N > 1$) as in the single stage version ($N = 1$). For a single stage, it was observed that a gas-liquid mixture fed at the top near the axis immediately separates into gas-liquid film flow. It is therefore expected that the gas-liquid flow that leaves the first stage also results in gas-

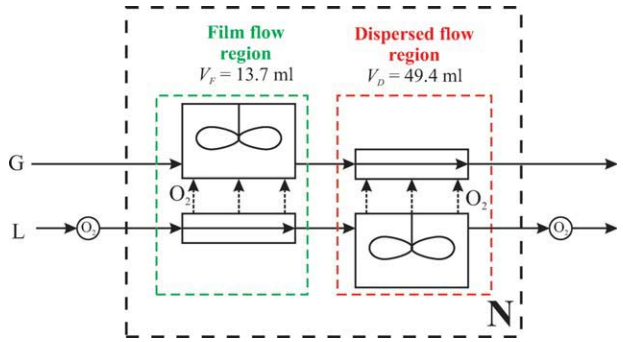

Figure 3. The reactor model of the multistage spinning disc reactor[2].

In the film flow region (see Figure 1), gas is ideally mixed and liquid is in plug flow, in the dispersed region, the gas phase is in plug flow and the liquid phase is ideally mixed. The gas and the liquid from the dispersed region of the 1st stage flow to the film flow region of the next stage. The number of stages, N, is 1, 2, or 3 in this study. The oxygen concentration is measured in the liquid phase at the inlet and at the outlet. [Color figure can be viewed in the online issue, which is available at wileyonlinelibrary.com.]

liquid film flow on top of the discs in the second and third stages. The reactor model as presented in Figure 2 is thus valid again but now the sequence is executed N times. The concentrations in the film flow region are calculated using a time dependent differential equation for the ideally mixed gas phase, coupled with a differential equation for the liquid, which is in plug flow. The exit concentrations of the phase are the input concentrations of the dispersed flow region, where the differential equation of the ideally mixed liquid phase is coupled with the differential equation of the gas phase. This procedure gives the output concentration as a function of time. The steady state value of the calculated concentration is fitted to the experimentally measured outlet concentration, with the value of $k_{GL}a_{GL}$ in the dispersed flow region as fitting parameter.

Results and Discussion

Gas-liquid mass transfer

Figure 4 shows the volumetric gas-liquid mass transfer coefficient in the dispersed flow region as a function of the rotational disc speed. Figure 4a shows the values with a 2-stage rotor-stator spinning disc reactor. The volumetric mass transfer increases with increasing rotational disc speed, which was also observed in the single stage unit.[2] An increase in gas flow rate leads to an increase in mass transfer as well. The same trends are observed in Figure 4b, for the 3-stage spinning disc reactor. At rotational disc speeds above 80 rad s^{-1}, however, the increase in mass transfer as a function of rotational disc speed seems to level off, and the mass transfer even decreases at higher rotational disc speeds. The leveling off and the decrease at higher rotational disc speeds is explained as follows. The gas-liquid mass transfer rates in the multistage spinning disc reactor are high, which means that equilibrium between the gas and the liquid will be reached at high rotational disc speeds. The measured oxygen concentration, however, is not exactly the same as the oxygen concentration in the gas phase calculated with the mass balance, but a little bit (between 0.001 and 0.005 mol m^{-3}) higher, due to a bias in the measurements. This slight overestimation of the oxygen concentration is probably due to the calibration method used, and only has a significant effect when the gas and the liquid are near equilibrium. The mass transfer rate is thus underestimated, and gets constant with increasing rotational disc speed. The value of the mass transfer in the film flow region, however, calculated with Eqs. 5 and 6 will increase with increasing rotational disc speed. This thus leads to a decrease in the volumetric gas-liquid mass transfer coefficient in the dispersed flow region. The

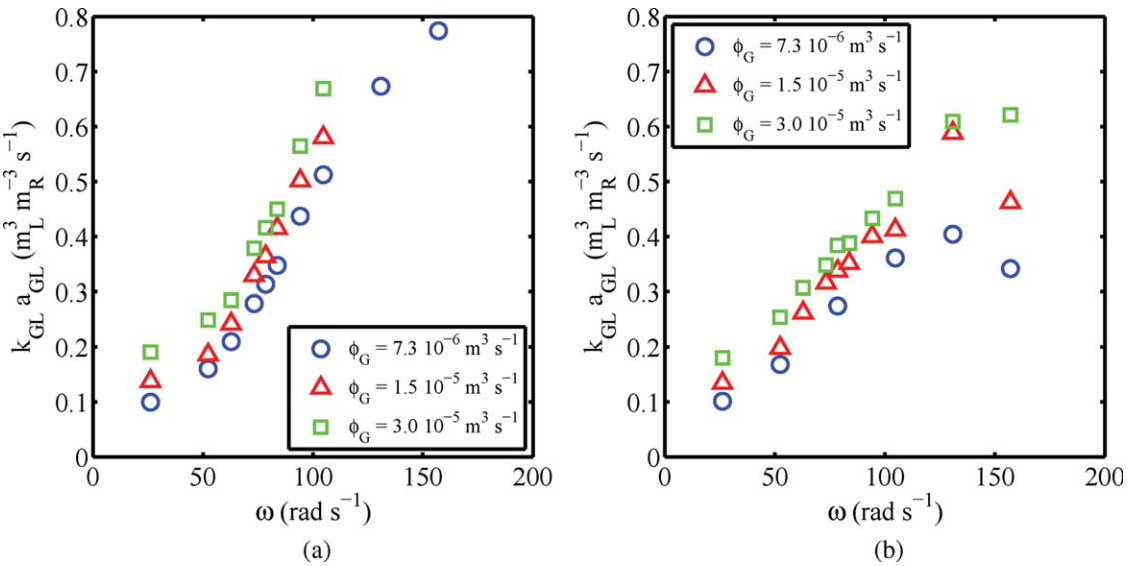

Figure 4. The volumetric gas-liquid mass transfer coefficient in the dispersed flow region, for a 2-stage reactor (a) and a 3-stage reactor (b), for various gas flow rates.

[Color figure can be viewed in the online issue, which is available at wileyonlinelibrary.com.]

measurements where the gas and the liquid concentrations are too close together are therefore discarded, if $(C_L^{out} - \frac{RT}{H}C_G^{out}) < 0.01$ mol m^{-3}.

The effect of the bias in the measurements is obviously larger if the number of stages increases. In the single stage spinning disc reactor the decrease of mass transfer coefficient was not observed, up to the maximum rotational disc speed of 180 rad s^{-1} used.[2] The method used, the desorption of oxygen from water, is thus not suitable to measure the gas-liquid mass transfer at rotational disc speeds higher than 80 rad s^{-1} for a 3-stage spinning disc reactor. The problem that the gas and the liquid reach equilibrium at higher rotational disc speeds can be overcome by using a (fast) reaction in the liquid bulk, which keeps the bulk concentration in the liquid low, preferably at a concentration of zero.

Figure 5 shows the volumetric gas-liquid mass transfer coefficient in the dispersed flow region, for the single stage, 2-stage and 3-stage rotor-stator spinning disc reactor. The values of $k_{GL}a_{GL}$ are equal for the 2-stage and the 3 stage reactor below 80 rad s^{-1}. Above this value, the increase with the 3-stage reactor levels off, which is due to the measurement method, as explained before. The values obtained in the single disc reactor are approximately the same, and follow the same trend, although the steep increase in mass transfer as a function of rotational disc speed starts at a somewhat higher rotational disc speed. The values for the single stage spinning disc reactor are obtained in a different setup,[2] since it was not possible to use one stage in the setup used in this study. The setup used by Meeuwse et al.[2] was of similar dimensions, it only had a rotating disc with a thickness of 4 mm instead of 6 mm. The measurements were performed at the same gas flow rate but at a lower liquid flow rate of $\phi_L = 6.7 \cdot 10^{-6}$ m^3 s^{-1}.

The fact that the obtained mass transfer coefficients are of the same magnitude as in the single disc system, is a strong indication that the gas-liquid flow (liquid film on rotor, gas bubbles dispersed in the rest of the reactor) is the same, for 2 or 3 stages. Unfortunately, no measurements for the multistage system could be done above 110 rad s^{-1}, due to the high mass transfer rates. At higher rotational disc speeds, it can thus not be shown that the same flow configuration is obtained, but it is plausible that the behavior will be the same. The co-fed rotor-stator spinning disc reactor can thus be scaled up by stacking multiple rotor-stator stages in series, where every stage has the same mass transfer performance as in a single stage reactor.

Energy dissipation rate

Figure 6a shows the energy dissipation in the spinning disc reactor as a function of rotational disc speed, for the 1, 2, and 3-stage spinning disc reactor. The energy dissipation rate is approximately equal for the 1, 2, and 3-stage reactor, which is another indication that the flow is the same in all stages. The energy dissipation rate decreases with 20% in the presence of gas, as shown in Figure 6b, the gas flow rate does not have an influence. A decrease in energy dissipation rate is expected, since a significant part of the reactor is filled with gas, which has a lower density and viscosity, and thus less energy is needed to accelerate the fluid. Figure 6b also shows the correlation for the energy dissipation for single phase flow in a rotor-stator spinning disc reactor from Daily and Nece.[8] The

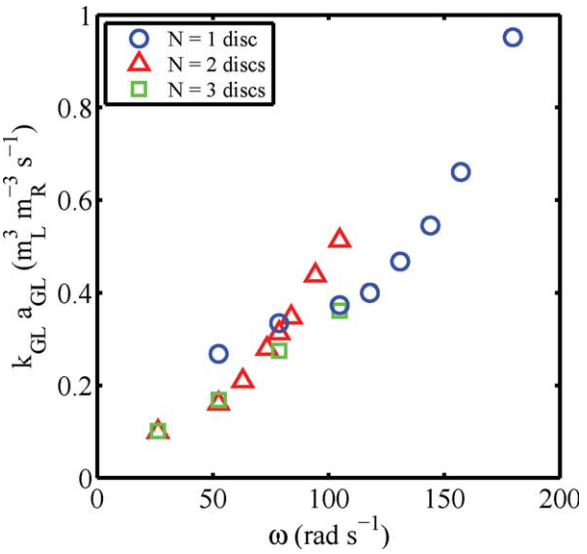

Figure 5. The volumetric gas-liquid mass transfer coefficient in the dispersed flow region, for a single stage, 2-stage, and 3-stage rotor-stator spinning disc reactor, at a gas flow rate of $7.3 \cdot 10^{-6}$ m^3 s^{-1}.

[Color figure can be viewed in the online issue, which is available at wileyonlinelibrary.com.].

values obtained in the single phase multistage rotor-stator spinning disc reactor are a factor 2.7 higher than those obtained from the correlation. This could be caused by the higher liquid throughflow rates used in this article. The ingoing liquid has to be accelerated to the velocity of the rotor, leading to a higher energy input. However, this is not experimentally proven, and no evidence of this is found in the literature.

Pressure

Figure 7 shows the pressure differences in the second stage of the 3-stage spinning disc reactor, with a liquid phase only (a), and with gas and liquid together (b). The pressure at the rim of the reactor is always higher than near the axis, due to the centrifugal pressure. The pressure thus increases from the axis on top of the disc to the rim of the reactor (ΔP_{top}), up to 1.0 bar at 459 rad s^{-1}. The pressure decrease between the rim of the reactor and the axis below the rotor (ΔP_{bottom}), is larger, up to 1.3 bar at 459 rad s^{-1}. The difference is the pressure drop per stage (ΔP_{stage}), which is thus up to 0.26 bar at 459 rad s^{-1}.

The pressure drop is not caused by the friction of the fluid, as would be the case in the flow between two flat plates. The centrifugal pressure plays a large role, as is seen by the influence of the rotational disc speed. The liquid flow rate has a large influence as well. The pressure drop per stage in the case of a liquid flow rate which is a factor 4 lower ($\phi_L = 6.7 \cdot 10^{-6}$ m^3 s^{-1}), is 0.024 bar at 459 rad s^{-1}, which is an order of magnitude lower. $\Delta P_{top} = 1.1$ bar, at 459 rad s^{-1}, in this case, and ΔP_{bottom} is thus almost the same. If no liquid flow rate would be present, no pressure drop over a stage would be expected of course, since the buildup of centrifugal pressure is then the same above the rotor as below the rotor. In the case of a (large) liquid flow

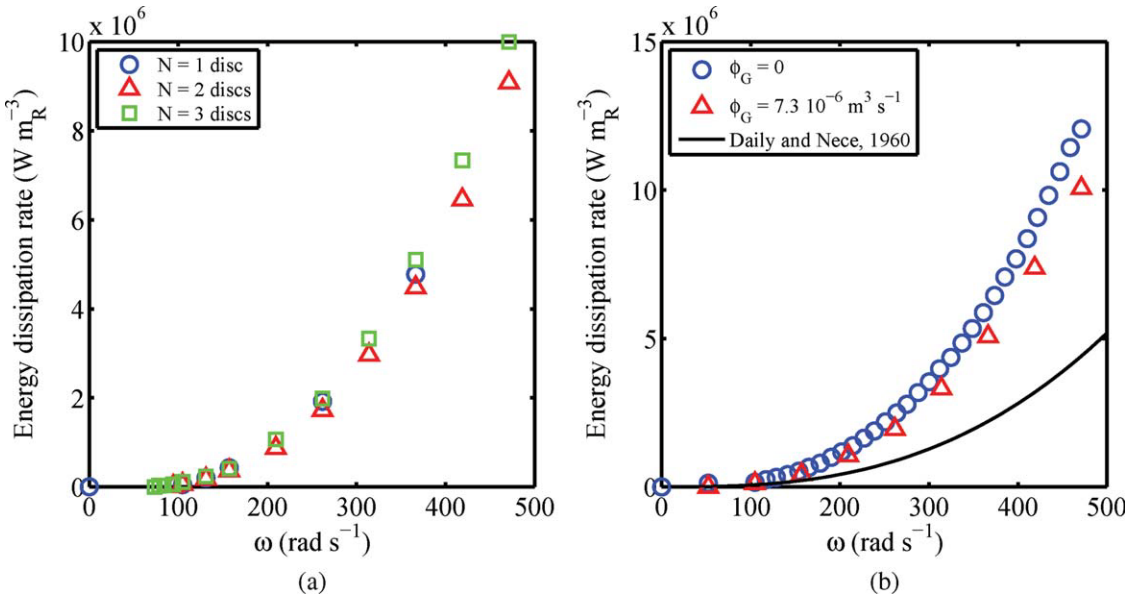

Figure 6. The energy dissipation rate in the multistage spinning disc reactor as function of the rotational disc speed.

(a) The energy dissipation rate for the single stage, 2-stage, and 3-stage reactor. (b) The energy dissipation rate for a 3 stage reactor with and without gas flow. The results of the correlation by Daily and Nece[8] are shown as well. [Color figure can be viewed in the online issue, which is available at wileyonlinelibrary.com.].

rate, the pressure buildup above the rotor will be lower, due to the centrifugal flow, while the pressure will decrease more below the rotor, where the flow is centripetal.[9–11]

The region between the rotor and the top stator is mainly filled with gas in the case of co-feeding of gas and liquid. The liquid flows over the rotor as a liquid film. The region between the rotor and the bottom stator is filled with liquid, with small gas bubbles dispersed in it. The gas holdup in the bottom part will thus be much lower than in the top part. The centrifugal pressure strongly depends on the density of the phases, ΔP_{top} will thus be much smaller than ΔP_{bottom}, as shown in Figure 7, with values of 0.33 bar and 0.97 bar at 459 rad s^{-1}. The resulting pressure drop per stage is thus 2.5 times higher than in the case with liquid only, with 0.64 bar at 459 rad s^{-1}.

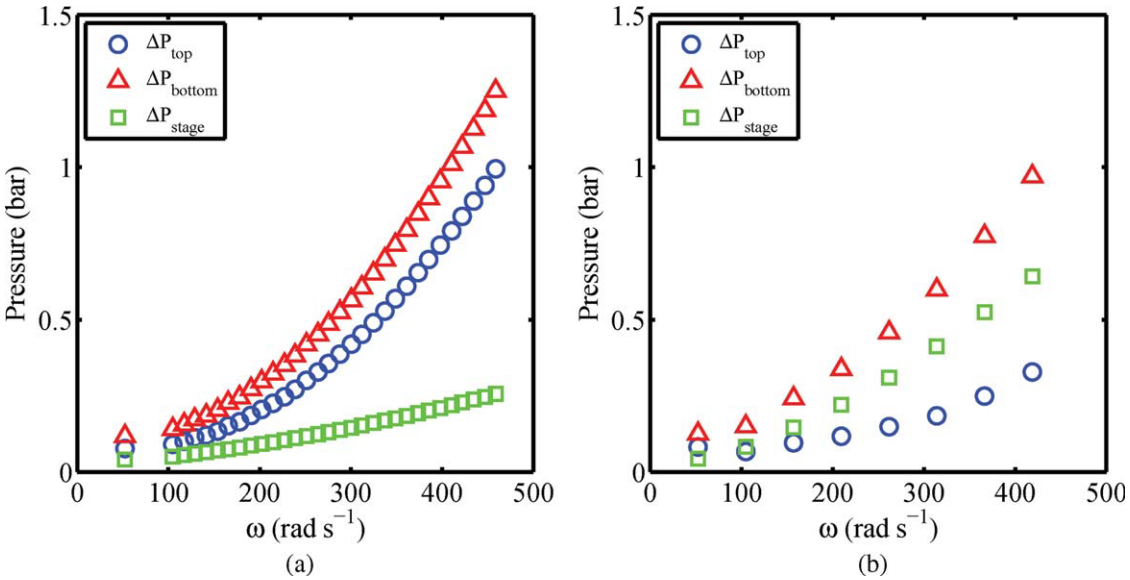

Figure 7. The pressure differences in the second stage of the 3-stage spinning disc reactor.

The pressures differences are denoted in Figure 2 and are: the pressure increase from the axis on top of the rotor toward the rim of the reactor, the pressure decrease from the rim of the reactor to the axis below the rotor, and the pressure drop over the stage, which is the difference between the two. The values are for the middle stage of the 3-stage reactor, with a liquid flow rate of $2.7 \cdot 10^{-5}$ m^3 s^{-1} (a) The pressures in the case of liquid only. (b) The pressures in case of liquid flow and a gas flow rate of $7.3 \cdot 10^{-6}$ m^3 s^{-1}. [Color figure can be viewed in the online issue, which is available at wileyonlinelibrary.com.]

Energy is needed to overcome the pressure drop in the reactor. This energy input also has to be taken into account in the total energy dissipation rate of the system. The energy needed to pressure the liquid, for a 3-stage reactor with a pressure drop of $1.9 \cdot 10^5$ Pa, follows from the work applied:

$$E_{d,L} = \frac{\int_{P_{atm}}^{P_0} \phi_L dP}{V_R} = \frac{\phi_L (P_{atm} - P_0)}{V_R} = 2.7 \cdot 10^4 \mathrm{W m_R^{-3}} \quad (7)$$

The isentropic work for compression can be used for the gas phase, assuming the ideal gas law:

$$E_{d,G} = \frac{\int_{P_{atm}}^{P_0} \phi_G dP}{V_R} = \frac{\int_{P_{atm}}^{P_0} \frac{\dot{n}RT}{p} dP}{V_R} = \frac{\dot{n}RT \ln \frac{P_0}{P_{atm}}}{V_R} = \frac{P_{atm} \phi_G RT \ln \frac{P_0}{P_{atm}}}{V_R} = 1.7 \cdot 10^4 \mathrm{W m_R^{-3}} \quad (8)$$

The total energy dissipation rate resulting from the pressure drop is thus:

$$E_{d,\Delta P} = E_{d,L} + E_{d,G} = 4.4 \cdot 10^4 \mathrm{W m_R^{-3}} \quad (9)$$

This is two orders of magnitude lower than the energy dissipation rate due to the rotation of the rotor and can therefore be neglected.

Reactor comparison

The rotor-stator spinning disc reactor has advantages and disadvantages, compared with conventional reactor equipment. The following sections describe the most important characteristics of the spinning disc reactor, and compares it with conventional reactors. The choice of a reactor for a certain process depends on the characteristics of the process; examples are presented of processes where the spinning disc is a suitable alternative for reactors commonly used in industry.

Mass transfer

The mass transfer coefficients presented in this paper for the multistage rotor-stator spinning disc reactor are only up to a rotational disc speed of 110 rad s^{-1}. It is shown that the single disc behavior repeats itself at each stage, and that scale-up by stacking rotor-stator units is possible. The mass transfer coefficient in a single stage rotor-stator spinning disc reactor is measured up to a rotational disc speed of 180 rad s^{-1}. The volumetric mass transfer coefficient in the film flow region is up to 0.4 m_L^3 m_R^{-3} s^{-1}, in the dispersed phase is it up to 0.95 m_L^3 m_R^{-3} s^{-1}.[2] This is 3 to 7 times higher than in conventional reactors such as bubble columns or stirred tank reactors.[12,13] The same mass transfer behavior is thus expected for the multistage spinning disc reactor. It is shown for the spinning disc reactor with a single gas inlet that the mass transfer coefficient can be increased even further by increasing the rotor size; an increase in rotor radius of a factor 2 leads to a 3-fold increase in mass transfer (Meeuwse et al. submitted). Additionally, the liquid-solid mass transfer coefficient is, with a value of $8 \cdot 10^{-4}$ m_L^3 m_i^{-2} s^{-1} at a rotational disc speed of 157 rad s^{-1}, an order of magnitude higher than, e.g., in a packed bed reactor.[14] The liquid-solid interfacial area, which can be up to 2000 m^2 m_R^{-3} is comparable or even higher than in this type of conventional reactor.

Heat transfer

From literature, it is known that the heat transfer coefficients in a rotor-stator system like the one used in this study, are up to $2 \cdot 10^4$ W m^{-2} K^{-1},[15] where the heat transfer toward the rotor is commonly up to 50% higher than to the stator.[16,17]. This is up to an order of magnitude higher than in conventional reactors, such as stirred tanks, bubble columns, and packed bed reactors. The interfacial area available for heat transfer is much higher than in conventional systems, if the rotor and the stator are used it can be up to 2000 m^2 m_R^{-3}. The overall heat transfer coefficient is therefore expected to be one or two orders of magnitude higher. The (multistage) rotor-stator spinning disc reactor is thus very promising for reactions where heat transfer plays a key role.

Energy requirements

This article shows the mass transfer coefficient in the multistage rotor-stator spinning disc reactor. The mass transfer rates obtained are high in comparison with conventional reactors. This is due to the high velocities, and the high degree of turbulence which is obtained in the rotor-stator spinning disc reactor. The energy input needed for the rotation of the rotors, together with the energy needed to overcome the pressure drop, influences the operation costs of this reactor. The energy dissipation rate in the spinning disc reactor is thus a factor that plays a significant role in the decision whether a spinning disc reactor will be chosen instead of a different type of reactor.

The maximum volumetric gas-liquid mass transfer coefficient obtained in the rotor-stator spinning disc reactor is approximately a factor 20 higher than the coefficient obtained for stirred tank reactors (Meeuwse et al., submitted).[18] The energy dissipation rate, however, is up to a factor 2000 higher than for this type of conventional equipment. The energy input is converted into heat and can thus be used to heat up the reactants, or this heat can be used for other process steps.

The rate of gas-liquid mass transfer per unit of energy dissipation ($\frac{k_{GL} a_{GL}}{E_d}$) is around 0.4 m_L^3 MJ^{-1} for a rotor with 0.135 m radius (Meeuwse et al., submitted) and 1.1 m_L^3 MJ^{-1} for a rotor with 0.066 m radius, while it is around 80 m_L^3 MJ^{-1} for a stirred tank reactor with a Rushton stirrer.[18] The mass transfer per unit of energy is thus much lower than for most conventional reactors.[19] The mass transfer coefficient, however, is much higher than for conventional equipment, as is shown in Figure 8.[19,20] A high mass transfer coefficient can have a large influence on the selectivity in the case of competitive or consecutive reactions. Mass transfer coefficients which are one order of magnitude higher, can give a new scope for reactions that were not economically feasible in conventional equipment, due to selectivity issues. The rotor-stator spinning disc reactor is thus mainly suited for this type of processes. Additionally, a large reduction in reactor size and volume can be achieved by using the rotor-stator spinning disc reactor, which can increase the safety of a process, due to the decreased inventory of (dangerous) chemicals. The smaller volume also makes it feasible to work at higher pressures, which opens a new window of reactor operation.

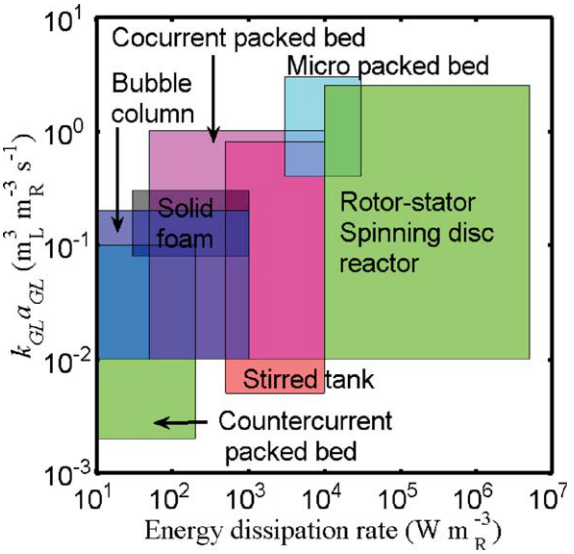

Figure 8. Volumetric mass transfer coefficient as function of energy dissipation, for a variety of multiphase reactors.[19,20]

The values of $k_{GL}a_{GL}$ obtained in the spinning disc reactor are more than one order of magnitude higher than in conventional reactor systems, however, the energy input is around 3 orders of magnitude higher. [Color figure can be viewed in the online issue, which is available at wiley onlinelibrary.com.]

Reactor operation

A single rotor-stator spinning disc reactor consists of a part where the gas is ideally mixed and the liquid is in plug flow (the film flow region) and a part where the gas is in plug flow and the liquid ideally mixed (dispersed flow region). For all positive order reactions, and thus also all reactions which are limited by mass transfer, which behave as a first order reaction, plug flow behavior is preferred. The ideally mixed regions in the spinning disc reactor are thus not beneficial. However, if the single stage reactor is expanded toward a multistage system, it behaves similarly to a cascade of mixers. If the number of stages is high enough, this mimics plug flow behavior.

Most of the conventional reactor systems that are used in industry which behave more or less as plug flow (e.g., packings or trickle bed reactors) have a mass transfer coefficient which is directly linked to the velocity in the reactor. Increasing the velocity gives a higher mass transfer rate, but this also decreases the residence time in the reactor. A longer column is then needed to get the same conversion. In a (multistage) rotor-stator spinning disc reactor the mass transfer is determined by the rotation of the discs and not by the flow rate of gas and liquid in the reactor. An extra degree of freedom is therefore present which is unavailable in most conventional systems.

Applications

The multistage rotor-stator spinning disc reactor requires more sophisticated equipment than conventional reactor systems. This will result in higher equipment costs and a higher risk of mechanical failure, due to the rotating parts. Apparatuses with rotating parts are widely used in industry (e.g., pumps or compressors), but they have higher costs for maintenance, to prevent failure of the mechanical parts. Additionally, the energy requirements are higher then for conventional equipment. The rotor-stator spinning disc reactor is therefore only economically attractive if the high heat and mass transfer rates justify the high investment and operational costs. This reactor is therefore probably not the best choice for large scale processes. Examples of processes in which the rotor-stator spinning disc reactor does have a large potential are given below.

An important advantage of the multistage rotor-stator spinning disc reactor is the high mass transfer rate, which significantly increases the conversion or decreases the reactor volume needed for a process. The smaller reactor volume thus has a lower amount of chemicals, which is especially beneficial in the case of dangerous reactants and/or products, since the risk of a spill or an explosion is decreased. For reactions at a higher pressure, a smaller reactor volume is also beneficial, since this decreases the outer surface area of the reactor. The gas holdup in the reactor is relatively low in the dispersed region (typically a few percent), and somewhat higher in the film flow region. For reactions with dangerous gases, this increases the safety even further. These aspects typically play a role in the production of pharmaceuticals and in fine-chemistry,[21,22] e.g., with hydrogenation, oxidation, and hydroformylation reactions. The energy dissipation rate, which is high in the spinning disc reactor compared with conventional reactors is not playing an important role in the total costs of these processes, especially in pharmaceutical industry, where time to market, selectivity, and conversion are much more important than the operation costs.

In parallel or serial reactions, the selectivity toward the desired product is an important issue. It is important to have a good control over the reactor conditions, especially if the mass transfer determines the selectivity. A (very) high mass transfer rate can have a positive influence on the selectivity; a (very) high energy dissipation rate is then not necessarily a problem. A higher selectivity can make a process economically feasible, e.g., since less separation effort is required.

Another potential application of the multistage rotor-stator spinning disc reactor is for highly exothermic reactions, since both the surface area and well as the heat transfer coefficient are high compared with other reactors. The formation of hot spots in the reactor is unlikely, since either the rotor or the stator is always close by. If the reaction is heterogeneously catalyzed and the catalyst is supported on the rotor and/or the stator, the heat can be removed locally, through the rotor and/or the stator.

Conclusions

The volumetric mass transfer coefficient in the dispersed flow region of a rotor-stator spinning disc reactor is the same for a single stage reactor, a 2-stage reactor and a 3-stage reactor. This proves the principle that the spinning disc reactor can be scaled up by using multiple rotor-stator units in series, where the rotors are mounted on a common axis. The gas-liquid mass transfer is measured up to a rotational disc speed of 100 rad s^{-1}, where the volumetric gas-liquid mass transfer coefficient is 0.7 m_L^3 m_R^{-3} s^{-1}. The mass transfer rates at higher rotational disc speeds could not be obtained, since the mass transfer is so high that the gas and liquid are virtually in equilibrium.

The pressure drop in the multistage spinning disc reactor increases with increasing liquid flow rate and rotational disc speed, up to 0.64 bar, at 459 rad s^{-1}. The pressure drop in the reactor is higher with the presence of gas and liquid then with liquid phase only.

The high mass and heat transfer rates, in combination with the high energy dissipation rate in the reactor, make the multistage rotor-stator spinning disc reactor mainly suitable for reactions with dangerous chemicals, reactions at high pressures, highly exothermic reactions and reactions where a significant increase in selectivity can be obtained due to the high mass transfer rates.

Acknowledgments

The authors gratefully acknowledge the financial support by the Dutch Technology Foundation STW and Alfa Laval. The support of DSM, Akzo Nobel, TNO, and MSD is also gratefully acknowledged.

Notation

a_{GL} = gas-liquid interfacial area, $m_i^2\ m_R^{-3}$
A_{top} = area on top side of the rotor, m_R^2
C = oxygen concentration mol, m_L^{-3}
C_w = flow rate coefficient, $C_w = \frac{\phi_L}{2\pi\nu R_D}$, –
D = diffusion coefficient in liquid, $m_L^2\ s^{-1}$
E_d = rate of energy dissipation, W m_R^{-3}
H = Henry coefficient, m_L^3 Pa mol^{-1}
h = rotor-stator distance, m_R
k_{GL} = gas-liquid mass transfer coefficient, $m_L^3\ m_i^{-2}\ s^{-1}$
$k_{GL}a_{GL}$ = volumetric gas-liquid mass transfer coefficient, $m_L^3\ m_R^{-3}\ s^{-1}$
$\dot{n}$ = molar gas flow rate, mol s^{-1}
N = number of stages, –
P_N = gauge pressure of stage, N Pa
R = gas constant, m_G^3 Pa $mol^{-1}\ K^{-1}$
R_D = Rotor radius, m_R
Re = Reynolds number, Re $= \frac{\omega R_D^2}{\nu}$, –
R_{ax} = radius of rotor axis, m_R
$\overline{Sh}$ = Sherwood number, $\overline{Sh} = \frac{\overline{k_{GL}}^{\frac{1}{3}}\left(R_D^2 - R_{ax}^2\right)}{D\left(R_D^{\frac{4}{3}} - R_{ax}^{\frac{4}{3}}\right)}$, –
Sc = Schmidt number, $Sc = \frac{\nu}{D}$, –
T = temperature K
V_D = volume dispersed flow region, m_R^3
V_F = volume film flow region, m_R^3
V_R = reactor volume, m_R^3

Greek letters

μ = dynamic viscosity, Pa s
ν = kinematic viscosity, $\nu = \frac{\mu}{\rho}\ m^2 s^{-1}$, –
ρ = density, kg m^{-3}
τ = torque, Nm
ϕ_G = gas flow rate at normal flow conditions, $m_G^3\ s^{-1}$
ϕ_L = liquid flow rate, $m_L^3\ s^{-1}$
ω = rotational disc speed rad, s^{-1}

Superscripts

out = outlet

Subscripts

atm = atmospheric
G = gas phase
L = liquid phase

Literature Cited

1. Meeuwse M, van der Schaaf J, Kuster BFM, Schouten JC. Gas-liquid mass transfer in a rotorstator spinning disc reactor. *Chem Eng Sci*. 2010;65:466–471.
2. Meeuwse M, van der Schaaf J, Schouten JC. Mass transfer in a rotor-stator spinning disk reactor with cofeeding of gas and liquid. *Ind Eng Chem Res*. 2010;49:1605–1610.
3. Meeuwse M, Lempers S, van der Schaaf J, Schouten JC. Liquid-solid mass transfer and reaction in a rotor-stator spinning disc reactor. *Ind Eng Chem Res*. 2010;49:10751–10757.
4. Aoune A, Ramshaw C. Process intensification: heat and mass transfer characteristics of liquid films on rotating discs. *Int J Heat Mass Transfer* 1999;42:2543–2556.
5. Peev G, Peshev D, Nikolova A. Gas absorption in a thin liquid film flow on a horizontal rotating disk. *Heat Mass Transfer* 2007;43:843–848.
6. Dijkstra D, van Heijst GJF. The flow between two finite rotating disks enclosed by a cylinder. *J Fluid Mech*. 1983;128:123–154.
7. Poncet S, Chauve MP, Gal PL. Turbulent rotating disk flow with inward throughflow. *J Fluid Mech*. 2005;522:253–262.
8. Daily JW, Nece RE. Chamber dimension effects on induced flow and frictional resistance of enclosed rotating Discs. *J Basic Eng-T ASME*. 1960;82:217–232.
9. Poncet S, Chauve MP, Schiestel R. Batchelor versus Stewartson flow structures in a rotor-stator cavity with throughflow. *Phys Fluids*. 2005;17:075110–075115.
10. Debuchy R, Dyment A, Muhe H, Micheau P. Radial inflow between a rotating and a stationary disc. *Eur J Mech B Fluids*. 1998;17:791–810.
11. Debuchy R, Nour FA, Bois G. On the flow behavior in rotor-stator system with superposed flow. *Int J Rotating Machinery*. 2008; 719510.
12. Van der Schaaf J, Chilekar VP, van Ommen JR, Kuster BFM, Tinge JT, Schouten JC. Effect of particle lyophobicity in slurry bubble columns at elevated pressures. *Chem Eng Sci*. 2007;62: 5533–5537.
13. Cents AHG, Brilman DWF, Versteeg GF. Ultrasonic investigation of hydrodynamics and mass transfer in a gas-liquid(-liquid) stirred vessel. *Int J Chem Reactor Eng*. 2005;3:A19.
14. Shah YT. *Gas-liquid-solid Reactor Design*. McGraw-Hill Inc.: London, 1979.
15. Owen JM, Haynes CM, Bayley FJ. Heat transfer from an air-cooled rotating disk. *Proc R Soc Lond. Ser A*. 1974;336:453–473.
16. Howey DA, Holmes AS, Pullen KR. Radially resolved measurement of stator heat transfer in a rotor-stator disc system. *Int J Heat Mass Transfer*. 2010;53:491–501.
17. Owen JM, Rogers RH. *Flow and Heat Transfer in Rotating-disc Systems*. Vol. 1. *Rotor-stator systems*. Taunton Research Studies Press, 1989.
18. Tschentscher R, Nijhuis TA, van der Schaaf J, Kuster BFM, Schouten JC. Gas-liquid mass transfer in rotating solid foam reactors. *Chem Eng Sci*. 2010;65:472–479.
19. Stemmet CP, Meeuwse M, van der Schaaf J, Kuster BFM, Schouten JC. Gas-liquid mass transfer and axial dispersion in solid foam packings. *Chem Eng Sci*. 2007;62:5444–5450.
20. Trambouze P, Euzen J-P. *Chemical Reactors*; 2004. 2nd ed. Paris, France: Editions Technip.
21. Chaudhari RV, Mills PL. Multiphase catalysis and reaction engineering for emerging pharmaceutical processes. *Chem Eng Sci*. 2004;59: 5337–5344.
22. Mills PL, Chaudhari RV. Reaction engineering of emerging oxidation processes. *Catal Today*. 1999;48:17–29.

Manuscript received Dec. 15, 2010, and revision received Jan. 23, 2011.